frontiers | Frontiers in Energy Research

TYPE Original Research
PUBLISHED 13 September 2022
DOI 10.3389/fenrg.2022.1010425

OPEN ACCESS

EDITED BY
Peng Li,
Tianjin University, China

REVIEWED BY
Haoran Ji,
Tianjin University, China
Weiyu Bao,
Shandong University, China

*CORRESPONDENCE
Yonggang Peng,
pengyg@zju.edu.cn

SPECIALTY SECTION
This article was submitted to Smart Grids, a section of the journal Frontiers in Energy Research

RECEIVED 03 August 2022
ACCEPTED 25 August 2022
PUBLISHED 13 September 2022

CITATION
Yang P, Peng Y, Xia Y, Wei W, Yu M and Feng Q (2022), A unified bus voltage regulation and MPPT control for multiple PV sources based on modified MPC in the DC microgrid.
Front. Energy Res. 10:1010425.
doi: 10.3389/fenrg.2022.1010425

A unified bus voltage regulation and MPPT control for multiple PV sources based on modified MPC in the DC microgrid

Pengcheng Yang, Yonggang Peng*, Yanghong Xia, Wei Wei, Miao Yu and Qifan Feng

The College of Electrical Engineering, Zhejiang University, Hangzhou, China

This study proposes a unified voltage regulation and maximum power point tracking (MPPT) method for photovoltaic (PV) sources in islanded direct current (DC) microgrids based on modified model predictive control (MPC). The method enables the PV sources to track the maximum power and serve as voltage sources for DC-bus voltage regulation when their available power is sufficient. Based on the proposed modified predictive model, the desired duty cycles can be calculated and directly applied to the PV sources in a constant switching frequency without a modulator. Real-time laboratory tests show that the PV sources can support the DC-bus voltage without energy storage (ES) and can proportionally share the load. Moreover, power oscillations and voltage ripples of the modified MPC get greatly attenuated compared with the traditional MPC under the same sampling frequency.

KEYWORDS

DC microgrid, maximum power point tracking (MPPT), model predictive control (MPC), photovoltaic (PV) sources, voltage regulation

1 Introduction

Currently, photovoltaic (PV) generation is becoming one of the most promising renewable power sources due to the continuous reduction in the cost of PV cells. Their DC output makes the DC microgrid an ideal solution to integrate distributed PV sources and supply local loads without the inversion stage (JacksonJusto et al., 2013; Dragičević et al., 2016; Kumar et al., 2017; Meng et al., 2017). A typical DC microgrid with multiple PV sources is shown in Figure 1. To make full use of solar energy, the maximum power point tracking (MPPT) method has been developed for PV sources in the past decades (Bollipo et al., 2020; Vicente et al., 2020). In DC microgrids, however, the maximum power output of PV sources may exceed the local demand and any available energy storage (ES) capacity, and the consequent power imbalance may result in DC-bus overvoltage and ES overcharging problems in the islanded model (Ullah et al., 2020).

Limiting the generation of PV sources is a common solution to these problems. Supported by centralized communication for collecting load data, limited generation of PV sources can be determined to balance the bus voltage (Wandhare and Agarwal, 2011).

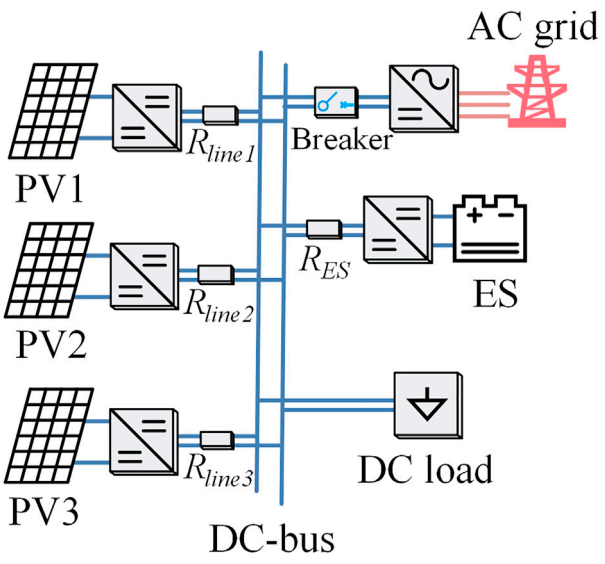

FIGURE 1
Dc microgrid with multiple PV sources.

Based on global information, a two-stage robust optimal PV dispatch model was proposed to satisfy the voltage constraints in case of the PV generation surplus load demand (Ding et al., 2017). In the study by Nguyen et al. (2019), combined with voltage regulators and switched capacitors, a comprehensive formulation of PV generation dispatch was studied to prevent the system from voltage violation and reverse power flow. Based on fast communication and global information, the abovementioned centralized PV generation regulation methods have heavy communication burdens and may suffer from a single point of failure.

The high cost and reliability concerns have motivated communication-free solutions. Based on the local DC bus signaling, a distributed mode switching strategy for the PV source was proposed (Tonkoski and Lopes, 2011; Ghosh et al., 2017). Once the bus overvoltage was detected, the MPPT controller was switched off, and the voltage regulation controller was motivated to linearly decrease the injected power until the bus voltage dropped to the rated value. However, the accompanying fluctuation deteriorated the bus voltage during the controller switching process. In the past years, droop-based control for PV sources has been successfully applied without a controller switch (Mahmood et al., 2015; Liu et al., 2016). Accordingly, the local DC-bus voltage is measured and utilized as feedback to regulate the PV operation point autonomously when the available maximum power is excessive. However, these controls are designed for cascaded converters with a two-stage structure and cannot be directly applied to one-stage structures. By introducing the dp/dv regulation loop, a $V - dp/dv$ droop control is designed to unify MPPT and voltage balance in one conversion stage (Cai et al., 2018a; Cai et al., 2018b). This improves the system efficiency compared with the two-stage structure; however, high precision sensors are required for the differential measurement.

Over the past decades, model predictive control (MPC) has been widely adopted to power electronics as a promising control method due to its robustness, excellent transient characteristics, and easiness to contain nonlinearities, constraints, and multi objectives (Quevedo et al., 2012; Dragičević, 2018). Instead of designing control loops and tuning parameters in traditional controls, a cost function is designed to evaluate the prediction and track the reference by minimizing the cost function in the MPC. In the study by Hu et al. (2019), a multi-objective MPC was designed for doubly-fed wind generators to regulate power and smooth grid connection; in addition, the controller was simple, without using any proportion integration (PI) regulators, current loops, and switching tables. The interrelations among the load current, circulating current, and capacitor voltages complicate the modular multilevel converters (MMCs) control. A weighted MPC based on a normalized cost function is proposed to achieve stable and balanced voltage and current control with reduced circulating current in various operating conditions for MMC (Ben-Brahim et al., 2016). In the study by Hu et al. (2021), a comprehensive review was present for individual and interconnected microgrids with MPC, which showed competitive advantages in bus voltage regulation, frequency recovery, and economic optimization compared with traditional controls. As for the PV sources, the former MPCs mainly focus on MPPT with a higher convergence speed under changing conditions and less ripple during the steady state (Lashab et al., 2018; Lashab et al., 2019). Still, voltage regulation with MPC is rarely studied for PV sources. In the study by Shadmand et al. (2014), MPPT and voltage regulation were realized by the inner MPPT-MPC and the outer droop-MPC, adopted separately on two cascaded converters. The voltage/current of PV sources cannot be obtained by the outer droop-MPC; hence, the desired power of the droop-MPC may not match the available power of PV sources. Therefore, voltage regulation needs to take the PV voltage/current into consideration in order to predict the available maximum power. The abovementioned MPCs emerged with a finite control set (FCS) appearance. It works with a variable switching frequency, which leads to a widespread harmonics spectrum for voltage/current waveforms, limiting the filter design and increasing the switching losses (Ahmad et al., 2018). As such, the continuous control set model predictive control (CCS-MPC) is designed and applied to a PV system with a constant switching frequency (Errouissi et al., 2016a; Errouissi et al., 2016b), while the voltage regulation is not involved in those research work.

TABLE 1 Comparison of control strategies.

Control strategies	MPPT	Voltage regulation	No controller transition	Constant switching frequency	No modulator	Applicable to multiple PV sources
Ref. Tonkoski and Lopes (2011) and Ghosh et al. (2017)	√	√		√		
Ref. Mahmood et al. (2015) and Liu et al. (2016)	√	√	√	√		√
Ref. Cai et al. (2018a) and Cai et al. (2018b)	√	√	√	√		√
Ref. Lashab et al. (2018)	√					√
Ref. Shadmand et al. (2014)	√	√	√		√	√
Ref. Ahmad et al. (2018) and Errouissi et al. (2016b)	√			√		√
The proposed control	√	√	√	√	√	√

In this study, a unified voltage regulation and MPPT control is designed for PV sources in islanded DC microgrids based on the modified MPC. With the proposed control, the PV sources can autonomously share power appropriately and regulate the DC-bus voltage without any energy storage or track the maximum power point (MPP) once their power output is not enough to feed the load. The comparison between the proposed method and the existing control methods is shown in Table 1, and the above superiorities are attributed to the following designed modifications:

1) By introducing the PV characteristics, a modified predictive model for PV sources is proposed for a more precise prediction; in addition, the desired duty cycles can be calculated and directly applied to the PV sources in a constant switching frequency without a modulator.
2) Taking both the operating point of PV sources and the DC-bus voltage into consideration, the unified PV current reference can be determined to regulate the DC-bus voltage when the available maximum power is redundant or track the maximum power point (MPP) when their power is not sufficient to feed the load.

A modified predictive model for PV sources is first proposed for a more precise prediction in Section 2, which modifies the duty cycle calculation of MPC. Then, the voltage regulation and MPPT are integrated according to the operating point of PV sources in Section 3, and the reference value is generated for MPC. According to the modified predictive model and generated reference value, the duty cycle is finally determined and adopted by the converters without modulation. HIL tests are conducted to verify the proposed control, and the comparisons and robustness tests are presented in Section 4.

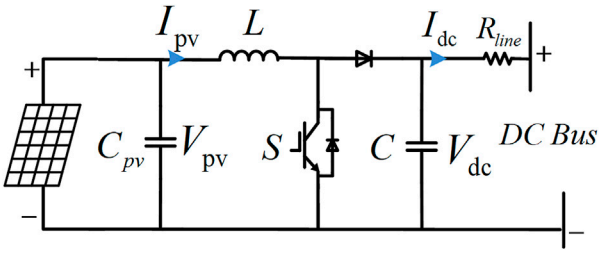

FIGURE 2
Topology of PV sources.

2 Modified MPC for PV sources

2.1 Review of FCS-MPC for PV sources

For the PV source in the DC microgrid, a boost converter–based model is studied, as shown in Figure 2, and its dynamic model can be written as

$$\begin{cases} L\dfrac{\mathrm{d}I_{pv}}{\mathrm{d}t} = V_{pv} - (1 - S(k))V_{dc} \\ C\dfrac{\mathrm{d}V_{dc}}{\mathrm{d}t} = (1 - S(k))I_{pv} - I_{dc} \end{cases}, \tag{1}$$

where $L$and C are the coefficients of the LC filter. V_{pv} and I_{pv} are the input PV voltage and PV current. V_{dc} and I_{dc} are the output DC voltage and DC current. $S(k)$ is the switching state of S at time k and is defined as

$$\begin{cases} S(k) = 1, & S\ is\ closed\ at\ time\ k \\ S(k) = 0, & S\ is\ open\ at\ time\ k \end{cases}. \tag{2}$$

To get the prediction value of PV sources, the discrete-time model is derived from Eq. 1 by using Euler's forward-difference law with sampling frequency $1/T$

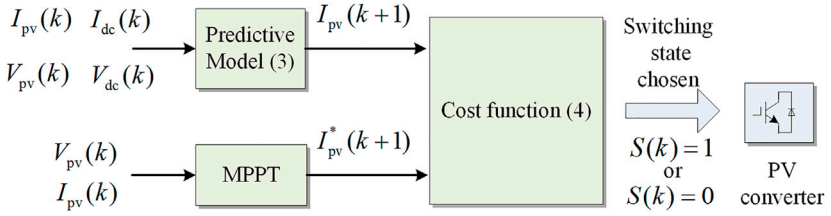

FIGURE 3
Traditional FCS-MPC for PV sources.

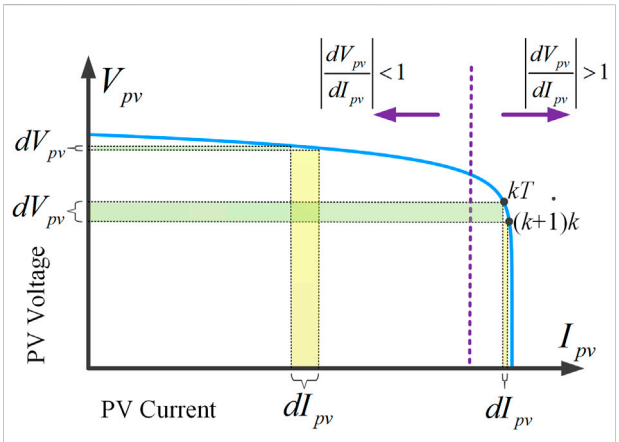

FIGURE 4
V-I characteristic of PV array.

$$\begin{cases} I_{pv}(k+1) = \dfrac{T}{L}\left[V_{pv}(k) - (1-S(k))V_{dc}(k)\right] + I_{pv}(k) \\ V_{dc}(k+1) = \dfrac{T}{C}\left[(1-S(k))I_{pv}(k) - I_{dc}(k)\right] + V_{dc}(k) \end{cases}, \quad (3)$$

where k denotes the present value at the sampling time kT, and k+1 denotes the predicted value at the next sampling time.

To evaluate the prediction, a cost function is defined as

$$g(k+1) = \left[I^*_{pv}(k+1) - I_{pv}(k+1)\right]^2, \quad (4)$$

where $I^*_{pv}(k+1)$ is the reference current at time instant $(k+1)T$, which is usually determined by the MPPT algorithm for the PV source. To minimize the cost function, the switching state with a closer prediction value to the reference value is chosen, and the traditional FCS-MPC scheme for PV sources is illustrated in Figure 3.

In the FCS-MPC,$V_{pv}(k)$ in Eq. 3 is considered as constant during sampling period T when predicting $I_{pv}(k+1)$. However, PV is actually not an ideal constant voltage source, and the variation of V_{pv} can be quite violent according to the V-I characteristic of the PV array in Figure 4. Comparing with the variation of I_{pv}, the variation of V_{pv} can be quite large, especially in the right segment of Figure 4. This may result in severe variation of V_{pv} during the sampling period T, and resultant deviation of the predicted $I_{pv}(k+1)$. In addition, maintaining the chosen switching state during the whole period can result in a relatively high voltage ripple, especially for low switching frequency conditions.

2.2 Modified MPC for PV sources

In the traditional FCS-MPC for PV sources, only the converter is modeled, and the model of PV array is rarely considered, which limits the accuracy of the predictive model. In this study, a more precise predictive model of PV sources is obtained by modifying $V_{pv}(k)$ of Eq. 3 to the average of $V_{pv}(k)$ and $V_{pv}(k+1)$, which can better formulate the contribution of V_{pv} from kT to $(k+1)T$. The updated prediction $I_{pv}(k+1)$ is

$$I_{pv}(k+1) = \frac{T}{L}\left[\frac{V_{pv}(k) + V_{pv}(k+1)}{2} - (1-S(k))V_{dc}(k)\right] + I_{pv}(k). \quad (5)$$

The V_{pv} at time $(k+1)T$ can be predicted as

$$V_{pv}(k+1) = V_{pv}(k) + m(k)\left[I_{pv}(k+1) - I_{pv}(k)\right], \quad (6)$$

where $m(k)$ is the slope of the V-I curve at the operating point $[I_{pv}(k), V_{pv}(k)]$. The one diode PV array model is adopted in this study, and its V-I characteristic can be expressed as

$$I_{pv} = N_P(I_{SC} + K_I\Delta T) \times \left[\frac{G}{G_N} - \frac{\exp\left(\frac{V_{pv}}{N_S V_t a}\right) - 1}{\exp\left(\frac{V_{OC}+K_V\Delta T}{V_t a}\right) - 1}\right], \quad (7)$$

where N_P and N_S are the numbers of parallel and series PV modules. I_{SC} and V_{OC} are the short-circuit current and open-circuit voltage of a PV module. G and G_N (1,000 W/m^2) are the actual irradiation and normal irradiation. ΔT is the difference between actual temperature T and normal temperature T_N (298.15 K). K_I and K_V are the current and voltage coefficients. $V_t = NkT_N/q$ is the thermal voltage of a PV module with Boltzmann constant k and electron charge q

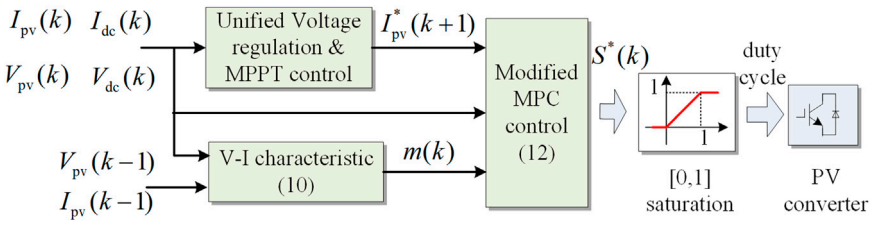

FIGURE 5
Proposed modified MPC for PV sources.

when T is close to T_N . N is the number of PV cells of a PV module. a is the ideality constant of the equivalent diode. The detailed explanations of PV modeling can be found in the study by Villalva et al. (2009).

According to Eq. 7, the slope $m(k)$ at the operating point $[I_{pv}(k), V_{pv}(k)]$ can be expressed as

$$m(k) = \frac{\exp\left(\frac{V_{OC}+K_V\Delta T}{V_t a}\right) - 1}{-N_P\left(I_{SC} + K_I\Delta T\right).\exp\left(\frac{V_{pv}(k)}{N_S V_t a}\right)/N_S V_t a}, \tag{8}$$

which costs a large computation. To simply the numerical computation, the former slope $m(k-1)$ at sampling time $(k-1)T$ is written as

$$\begin{aligned} m(k-1) &= \frac{\exp\left(\frac{V_{OC}+K_V\Delta T}{V_t a}\right) - 1}{-N_P\left(I_{SC} + K_I\Delta T\right)\bullet \exp\left(\frac{V_{pv}(k-1)}{N_S V_t a}\right)/N_S V_t a} \\ &= \frac{V_{pv}(k) - V_{pv}(k-1)}{I_{pv}(k) - I_{pv}(k-1)}. \end{aligned} \tag{9}$$

Comparing the two slopes in Eqs 8 and 9, the slope $m(k)$ can be simplified as

$$m(k) = \frac{V_{pv}(k) - V_{pv}(k-1)}{I_{pv}(k) - I_{pv}(k-1)} \exp\left(\frac{V_{pv}(k-1) - V_{pv}(k)}{N_S V_t a}\right). \tag{10}$$

Combining Eqs 5, 6, and 10, the modified predictive model with the PV characteristic can be written as

$$I_{pv}(k+1) = \frac{2T}{2L - Tm(k)}\left[V_{pv}(k) - (1 - S(k))V_{dc}(k)\right] + I_{pv}(k). \tag{11}$$

Once $I_{pv}(k+1)$ is equal to $I^*_{pv}(k+1)$ in Eq. 4, the cost function is minimal. According to Eq. 11, the desired $S^*(k)$ to make $I_{pv}(k+1)$ equal with $I^*_{pv}(k+1)$, can be calculated as

$$S^*(k) = \frac{2L - Tm(k)}{2T}\left[I^*_{pv}(k+1) - I_{pv}(k)\right] - \frac{V_{pv}(k)}{V_{dc}(k)} + 1. \tag{12}$$

By limiting $S^*(k)$ to [0,1], the resulting $S^*(k)$ can be set as a duty cycle and directly applied to PV sources. Instead of choosing the switching state between 0 and 1, the proposed control can reduce the voltage ripple in a constant switching frequency without a modulator. The overall control topology is shown in Figure 5. The reference $I^*_{pv}(k+1)$ is obtained by the unified voltage regulation and MPPT control, which is detailed in the next section. With the proposed modified MPC, the PV sources can track the reference accurately.

3 Unified voltage regulation and MPPT control for PV sources

3.1 Voltage regulation control

For the PV sources, the participation in voltage regulation has been an increasing demand for the islanded DC microgrid system. The droop control is commonly adapted to regulate the voltage and share the load among multi-sources. In the predictive model, the droop control can be expressed as

$$V^*_{dc}(k+1) = V^* - nI_{dc}(k), \tag{13}$$

where $V^\star$ and n are the normal DC voltage and the droop coefficient. $V^*_{dc}(k+1)$ is the reference DC-bus voltage in the next sampling time The predicted output power of PV source can be written as

$$P^{Vbus}_{out}(k+1) = V^*_{dc}(k+1)\cdot I_{dc}(k). \tag{14}$$

To maintain the reference DC-bus voltage $V^*_{dc}(k+1)$, the charging power for capacitor C can be calculated as

$$P^{Vbus}_{charge}(k+1) = \frac{1}{M}\cdot\frac{1}{T}\left[\left(0.5C\cdot V^*_{dc}(k+1)^2 - 0.5C\cdot V_{dc}(k)^2\right)\right], \tag{15}$$

where M is a filter coefficient to limit the capacitor's charging power. In the voltage regulation control, the required power of the PV source is the sum of output power and charging power. According to the power balance, the provided power $P^{Vbus}_{in}(k+1)$ by the PV array can be written as

$$\begin{aligned} P^{Vbus}_{in}(k+1) &= I^{Vbus}_{pv}(k+1)\cdot V_{pv}(k) \\ &= P^{Vbus}_{out}(k+1) + P^{Vbus}_{charge}(k+1), \end{aligned} \tag{16}$$

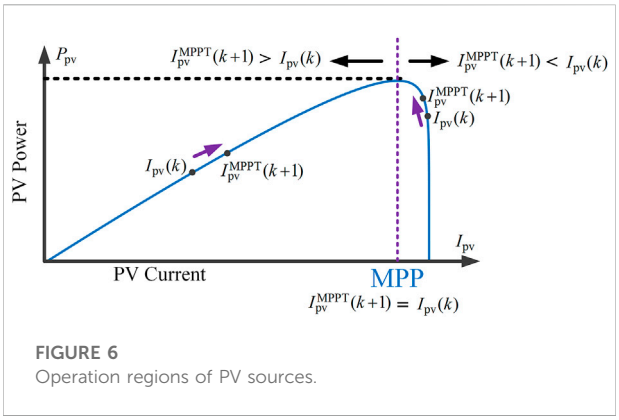

FIGURE 6
Operation regions of PV sources.

where $I_{pv}^{Vbus}(k+1)$ is the reference PV current in the next sampling time for the voltage regulation control. Combining Eq. 13 to Eq. 16, $I_{pv}^{Vbus}(k+1)$ can be calculated as

$$I_{pv}^{Vbus}(k+1) = \frac{1}{V_{pv}(k)}\left\{\left[V^* - nI_{dc}(k)\right]\cdot I_{dc}(k) + \frac{C}{2MT}\left[(V^* - nI_{dc}(k))^2 - V_{dc}(k)^2\right]\right\}. \quad (17)$$

By setting the $I_{pv}^{*}(k+1)$ in Eq. 12 as the $I_{pv}^{Vbus}(k+1)$ in Eq. 17 and adopting the corresponding duty cycle $S^*(k)$ of Eq. 12, the PV source can offer the required power to track the reference DC-bus voltage and behave like a DC voltage source.

3.2 Unified control for PV sources

Different from regulating the voltage of DC-bus, the MPPT control tries to extract the maximum power. The corresponding MPPT algorithm, such as Perturb and Observe (P&O) or incremental conductance (INC) method, can generate a reference current $I_{pv}^{MPPT}(k+1)$ for the PV source, which may be different from $I_{pv}^{Vbus}(k+1)$ generated by the voltage regulation control. By setting the $I_{pv}^{*}(k+1)$ in Eq. 12 as the $I_{pv}^{MPPT}(k+1)$ and adopting the corresponding duty cycle $S^*(k)$ of Eq. 12, the PV source can track the maximum power.

Another crucial contribution of this study is to unify voltage regulation and MPPT control. In the MPC-based control, the reference in the cost function plays a key role in determining the final behavior of the converter. In the proposed unified control, the coordination between DC-bus voltage regulation and MPPT is realized by selecting the corresponding voltage regulation reference $I_{pv}^{Vbus}(k+1)$ or MPPT reference in different PV conditions. In this study, the operation conditions of the PV sources are divided into three parts, as shown in Figure 6, and the corresponding reference selection mechanism is detailed as follows:

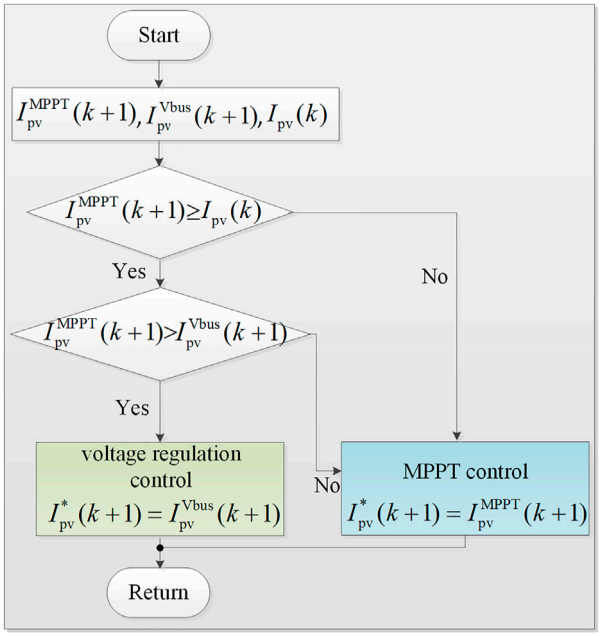

FIGURE 7
Flowchart of the reference selection mechanism.

(1)$I_{pv}^{MPPT}(k+1) > I_{PV}(k)$: In this case, the power output increases as the PV current increases, and the PV sources operate in the left region of Figure 6. If $I_{pv}^{MPPT}(k+1)$ is more than $I_{pv}^{Vbus}(k+1)$, the PV sources can supply the power demand for the voltage regulation in the next time instant, and, hence, $I_{pv}^{*}(k+1)$ can be set as $I_{pv}^{Vbus}(k+1)$ to regulate the voltage. Conversely, if $I_{pv}^{MPPT}(k+1)$ is less than $I_{pv}^{Vbus}(k+1)$), the PV sources cannot supply the desired power for the voltage regulation in the next time instant, and $I_{pv}^{*}(k+1)$ should be $I_{pv}^{MPPT}(k+1)$ to maximize the power output.
(2)$I_{pv}^{MPPT}(k+1) = I_{PV}(k)$: In this case, the PV sources operate at the maximum power point (MPP). If $I_{pv}^{MPPT}(k+1)$ is more than $I_{pv}^{Vbus}(k+1)$, $I_{pv}^{*}(k+1)$ can be set as $I_{pv}^{Vbus}(k+1)$ to regulate the voltage. Conversely, if $I_{pv}^{MPPT}(k+1)$ is less than $I_{pv}^{Vbus}(k+1)$, it is impossible to extract more power from the PV sources by MPP, and $I_{pv}^{*}(k+1)$ should be $I_{pv}^{MPPT}(k+1)$ to obtain the maximum power output.
(3)$I_{pv}^{MPPT}(k+1) < I_{PV}(k)$: In this situation, the PV sources operate in the right region of Figure 6, which is also called the current-source zone (Xiao et al., 2007). In this segment the system becomes lightly damped, resulting in reduced power output and an inability to control effectively (Cai et al., 2018a; Xiao et al., 2007). Thus, this condition should be avoided, and operation in the left segment is preferred. $I_{pv}^{*}(k+1)$ is set as $I_{pv}^{MPPT}(k+1)$ to climb the MPP and then to reach the left segment.

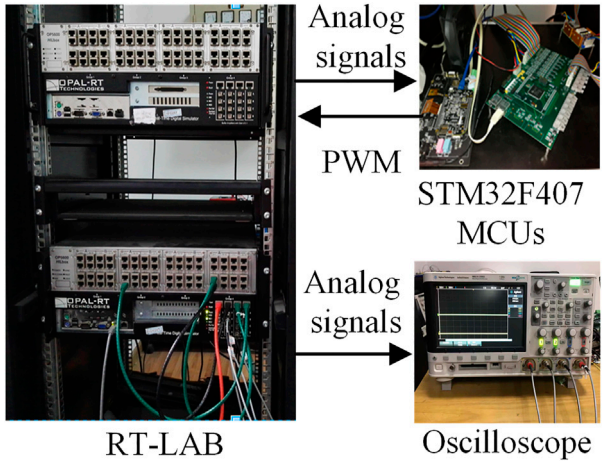

FIGURE 8
HIL test facilities.

Figure 7 shows the simplified flowchart of the aforementioned reference selection mechanism. By evaluating the reference values $I_{pv}^{Vbus}(k+1)$, $I_{pv}^{MPPT}(k+1)$, and $I_{PV}(k)$, the operation region can be determined, and the corresponding reference PV current $I_{pv}^{*}(k+1)$ in Eq. 12 can be finally chosen. With the proposed unified method and modified MPC in Figure 5, PV sources can regulate the bus voltage when the power demand can be satisfied, otherwise providing the maximum power. The participation of PV sources in voltage regulation reduces the use of ESs in the islanded microgrid, especially when the power output of the PV sources exceeds the demand. As such, the ESs can operate as back-up power to compensate for the demand when the PV power output is not sufficient, prolonging the lifetime of the ESs.

4 Verification and discussion

To verify the efficacy of the proposed unified control, the hardware in loop tests are conducted using RT-LAB and STM32F407MCUs, as shown in Figure 8. The DC microgrid with three PV sources, as shown in Figure 1, is tested. PVs' power output ratio is 1:1.38:1.78 under the same temperature and solar irradiation conditions. As such, their droop coefficients are set as 0.5 V/A, 0.36 V/A, and 0.28 V/A to proportionally share the load, and their normal DC voltage V^* is set at 200 V. An ES is connected at the DC-bus by a bidirectional DC/DC converter, and the traditional DC droop control is adopted to regulate its output voltage.

4.1 Bus voltage regulation test

Figure 9 shows the system responses under step-changes of the load and solar irradiation. In the initial State I, both the PV sources and the ES are connected to regulate the DC-bus voltage. In State II, the ES is disconnected from the DC-bus. The initial load $R = 10\Omega$ is changed to $R = 8\Omega$ in State III and further changed to $R = 5.7\Omega$ in State IV. In State V, the solar irradiation of PV1 increases from 800 W/m^2 to 1,200 W/m^2. In State VI, the solar irradiations of PV2 and PV3 increase from 800 to 1,200 W/m^2.

Figure 9A shows the power outputs of the PV sources and the ES, and Figure 9B shows the response of the DC-bus voltage. In State I, the ES absorbs the excessive PV power to maintain the power balance. In State II, the ES is removed, and the PV sources compensate their power outputs to maintain the DC-bus voltage without the ES. When the load increases in State III, the PV sources proportionally increase their power outputs. In State IV, the load further increases and exceeds the available maximum power. The PV sources provide their maximum power, which is still not sufficient to feed the load and maintain the DC-bus voltage, resulting in a 10.9% voltage drop. In State V, the power output of PV1 increases since its solar irradiation rises; however, the total power output of the PV sources is still not enough to maintain the DC-bus voltage. Thus, the PV sources track their MPPs, and the voltage drop is alleviated to 5.2%. In State VI, with the solar irradiations of PV2 and PV3 increasing, the total available maximum power is sufficient for the load demand, and the PV sources coordinately regulate the DC-bus voltage. The power sharing results in different states are listed in Table 2. It is shown that the power sharing ratio is close to the designed ratio of 1:1.38:1.78 under the same solar irradiation condition. If the solar irradiations of PV sources are different, the proposed control will not maintain the power output according to the sharing ratio when the power is not sufficient, which can make full use of solar energy and alleviate the DC-bus voltage deviation.

With the proposed unified control, the PV sources can regulate the DC-bus voltage when their available maximum power is sufficient; otherwise, track the MPP to compensate for the high load. The load can be shared proportionally according to the capacities of PV sources without communication links.

4.2 Comparison test

The MPPT and voltage regulation dynamic responses of PV sources with different control methods are compared in Figure 10. The solar irradiation increases from 800 to 1,200 W/m^2 in State II in order to test the MPPT dynamic

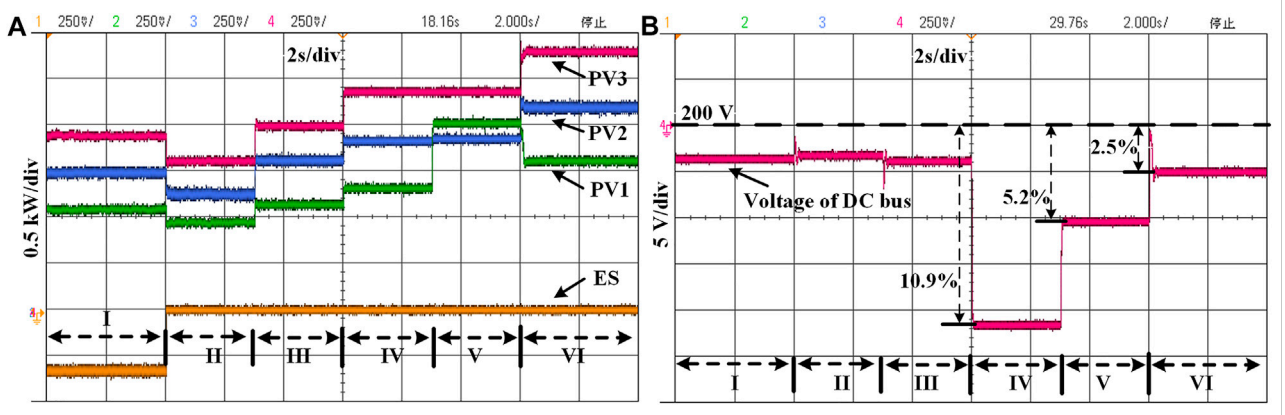

FIGURE 9
System responses under step-changed load and solar irradiation **(A)** Power outputs of PV1, PV2, PV3, and ES. **(B)** DC-bus voltage.

TABLE 2 Power outputs of three PV arrays.

State	PV1 (kW)	PV2 (kW)	PV3 (KW)	PV power ratio
I	1.15	1.53	1.95	1:1.33:1.70
II	0.94	1.28	1.60	1:1.36:1.70
III	1.17	1.62	2.02	1:1.38:1.73
IV	1.37 (MPP)	1.88 (MPP)	2.41 (MPP)	1:1.37:1.76
V	2.08 (MPP)	1.89 (MPP)	2.41 (MPP)	1:0.91:1.16
VI	1.63	2.20	2.83	1:1.35:1.74

response. The ES is removed in State III to test the dynamic response of the voltage regulation.

The comparison results are listed in Table 3. For the MPPT, a relatively high sampling frequency is preferred to restrain the power oscillation for the traditional MPC, which results in a heavy computation burden and a high switching frequency. The $V - dp/dv$ droop control in the study by Cai et al. (2018a) can efficiently extract the maximum power without a high-sampling frequency. However, based on the traditional multi-loop feedback topology, the response speed of $V - dp/dv$ droop control is much lower than the MPC, resulting in a longer MPPT time with varying solar irradiation. Based on the modified predictive model of PV sources, the proposed unified control can generate the duty cycle of each period to be directly used by the PV sources without a modulator. As such, the MPPT speed of the proposed unified control is much faster than the $V - dp/dv$ droop control. Compared with the traditional MPC, which applies one switching state during the whole sampling period, the duty cycle control can modify the duration of the switching states in one sampling period, which greatly reduces ripple. For voltage regulation, the traditional MPC cannot regulate the voltage when the power outputs of PV sources are sufficient, resulting in a DC-bus voltage rise in State III. The $V - dp/dv$ droop control can maintain the voltage; however, the dynamics of the DC-bus voltage are not satisfactory, with a 17.2% overshoot. The proposed unified control can regulate the DC-bus voltage and constrain the overshoot and the voltage ripples.

4.3 Robustness test

The mismatch of the predictive model can affect the performance of MPC, which may lead to an undesirable duty cycle for MPPT and voltage regulation in the PV sources. A robustness test for the proposed unified control with mismatched parameters (L and C) is shown in Figure 11. As observed, the mismatch of C has little impact on the system responses, which is actually more influenced by the mismatch of L. As shown in Eq. 5, the current prediction can be affected by the L, while the C has no influence on the current

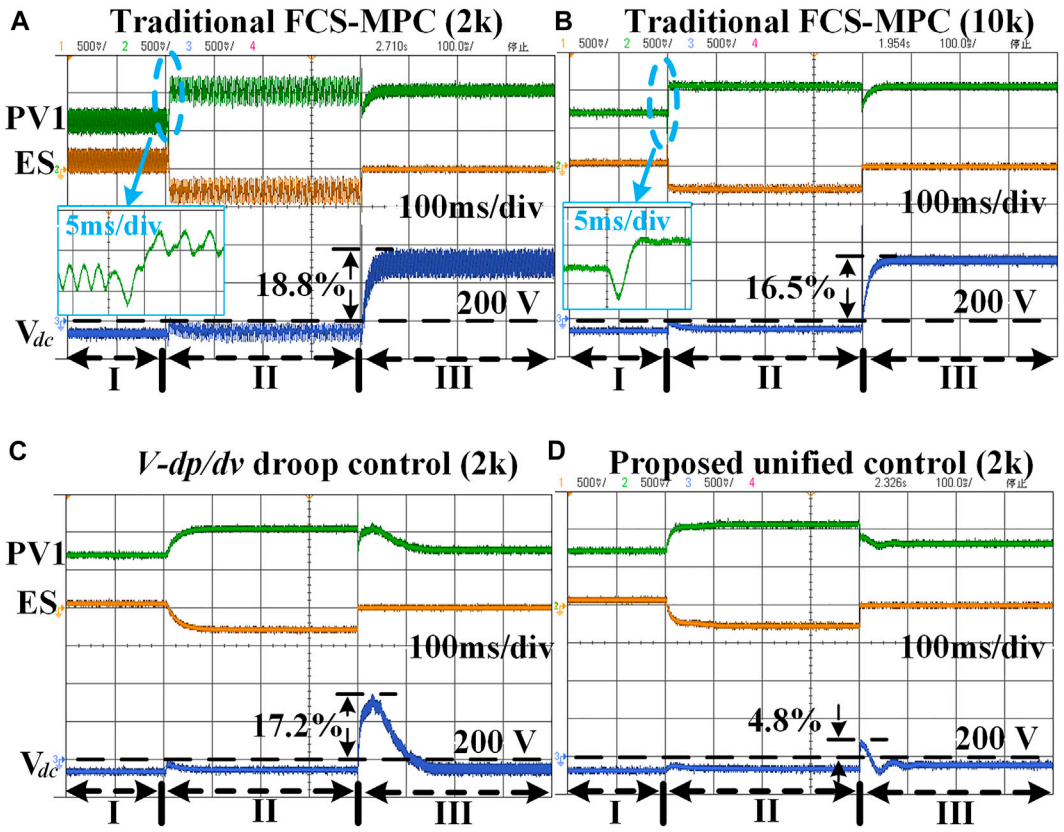

FIGURE 10
Comparisons of the MPPT and voltage regulation dynamic responses with different control methods for PV1. **(A)** Traditional MPC with a 2 kHz sampling frequency. **(B)** Traditional MPC with a 10 kHz sampling frequency. **(C)** Unified control based on $V - dp/dv$ droop control with a 2 kHz sampling frequency. **(D)** Proposed unified control with a 2 kHz sampling frequency.

TABLE 3 MPPT and voltage regulation dynamic responses with different controls.

Control method	MPPT (State I and II)			Voltage regulation (State III)		
	MPPT efficiency (%)	Tracking time (ms)	Power ripples (%)	Maximum overshoot (V)	Voltage deviation	Voltage ripples (%)
Traditional MPC (2k)	98.6	8	40.4	37.6	31.5 V	6.1
Traditional MPC (10k)	99.9	4	3.8	33.0	31.5 V	1.5
$V - dp/dv$ droop control (2k)	99.8	45	3.6	34.4	−3.1 V	2.2
Proposed unified control (2k)	99.9	18	2.6	9.6	−3.1 V	1.1

prediction. The detailed influence of the mismatched L on the MPPT and voltage regulation is shown in Figure 12. It can be seen that the voltage shows better robustness than the maximum power output, and both the maximum power output and DC-bus voltage have a better tolerance to the small-mismatched L than the large-mismatched L.

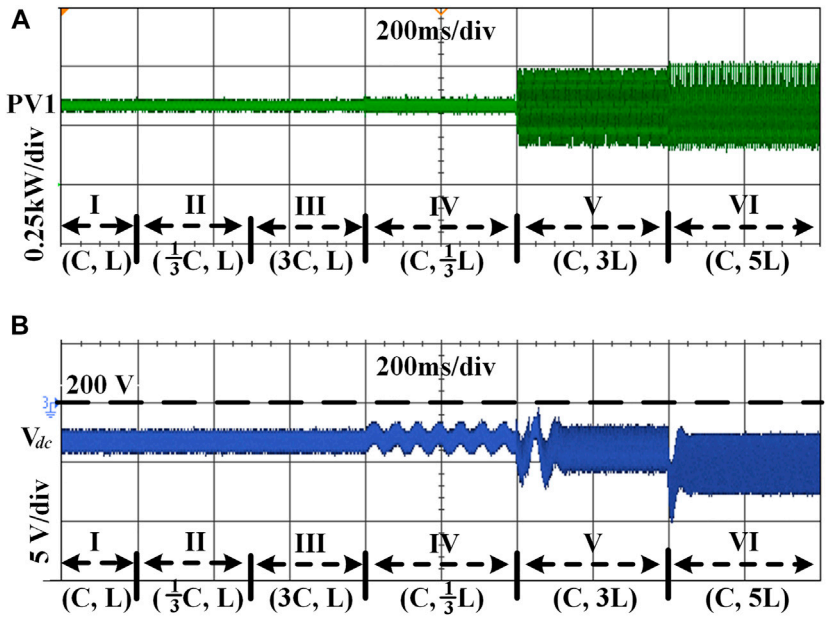

FIGURE 11
Robustness test with model parameter mismatches. **(A)** Power output of PV1 with mismatched C and L. **(B)** DC-bus voltage with mismatched C and L.

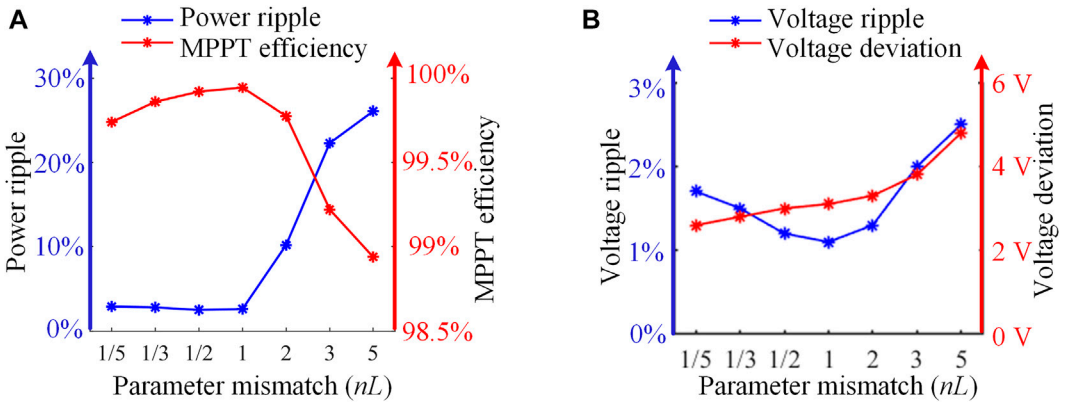

FIGURE 12
Influences of the mismatched *L* on the maximum power output and voltage regulation. **(A)** The influence on the MPPT. **(B)** The influence on the voltage.

5 Conclusion

In this study, a unified voltage regulation and MPPT control is designed for PV sources based on modified MPC. The PV sources can autonomously regulate the DC-bus voltage when the available maximum power is redundant or track the maximum power when their power outputs are not sufficient. The modified MPC can generate the duty cycle, which is adopted by the PV sources under constant switching frequency without a modulator. The HIL test results show that the PV sources can regulate the DC-bus voltage without ES and can proportionally share the load. In general, according to the comparison and robustness tests, the proposed unified control is suitable for PV sources without high switching frequency and can efficiently accommodate the rapidly varying illumination and load conditions. The ongoing study will further improve the credibility and reliability of the proposed control under

all possible conditions, such as partial shading and bus voltage sags and surges.

Data availability statement

The original contributions presented in the study are included in the article/Supplementary Material; further inquiries can be directed to the corresponding author.

Author contributions

All authors listed have made a substantial, direct, and intellectual contribution to the work and approved it for publication.

Funding

This work is supported in part by the National Key R&D Program of China (2020YFB1506801), the Science and Technology Project of the State Grid Corporation of China (52110421005H), the National Natural Science Foundation of China (52007162 and 51877188), the Key R&D Program of Zhejiang Province (2022C01161), the China Postdoctoral Science Foundation (2022M712727), and the Fundamental Research Funds for the Central Universities (226-2022-00053).

Conflict of interest

The authors declare that the research was conducted in the absence of any commercial or financial relationships that could be construed as a potential conflict of interest.

Publisher's note

All claims expressed in this article are solely those of the authors and do not necessarily represent those of their affiliated organizations, or those of the publisher, the editors, and the reviewers. Any product that may be evaluated in this article, or claim that may be made by its manufacturer, is not guaranteed or endorsed by the publisher.

References

Ahmad, D, Farahani, G, Vahedi, H, and Al-Haddad, K (2018). Model predictive control design for DC-DC converters applied to a photovoltaic system. *Int. J. Electr. Power & Energy Syst.* 103, 537–544. doi:10.1016/j.ijepes.2018.05.004

Ben-Brahim, L., Gastli, A., Trabelsi, M., Ghazi, K. A., Houchati, M., and Abu-Rub, H. (2016). Modular multilevel converter circulating current reduction using model predictive control. *IEEE Trans. Ind. Electron.* 63 (6), 3857–3866. doi:10.1109/tie.2016.2519320

Bollipo, R. B., Mikkili, S., and Bonthagorla, P. K. (2020). Critical review on PV MPPT techniques: Classical, intelligent and optimisation. *IET Renew. Power Gener.* 14 (9), 1433–1452. doi:10.1049/iet-rpg.2019.1163

Cai, H., Xiang, J., Wei, W., and Chen, M. Z. Q. (2018). Droop control for PV sources in DC microgrids. *IEEE Trans. Power Electron.* 33 (9), 7708–7720. doi:10.1109/tpel.2017.2771803

Cai, H., Xiang, J., and Wei, W. (2018). Decentralized coordination control of multiple photovoltaic sources for DC-bus voltage regulating and power Sharing. *IEEE Trans. Ind. Electron.* 65 (7), 5601–5610. doi:10.1109/tie.2017.2779412

Ding, T., Li, C., Yang, Y., Jiang, J., Bie, Z., and Blaabjerg, F. (2017). A two-stage robust optimization for centralized-optimal dispatch of photovoltaic inverters in active distribution networks. *IEEE Trans. Sustain. Energy* 8 (2), 744–754. doi:10.1109/tste.2016.2605926

Dragičević, T., Lu, X., Vasquez, J. C., Guerrero, J. M., and Dc Microgrids—Part, I. (2016). A review of control Strategies and stabilization techniques. *IEEE Trans. Power Electron.* 31 (7), 4876–4891. doi:10.1109/TPEL.2015.2478859

Dragičević, T. (2018). Model predictive control of power converters for robust and fast operation of AC microgrids. *IEEE Trans. Power Electron.* 33 (7), 6304–6317. doi:10.1109/tpel.2017.2744986

Errouissi, R., Al-Durra, A., and Muyeen, S. M. (2016). A robust continuous-time MPC of a DC–DC boost converter interfaced with a grid-connected photovoltaic system. *IEEE J. Photovolt.* 6 (6), 1619–1629. doi:10.1109/jphotov.2016.2598271

Errouissi, R., Muyeen, S. M., Al-Durra, A., and Leng, S. (2016). Experimental validation of a robust continuous nonlinear model predictive control based grid-interlinked photovoltaic inverter. *IEEE Trans. Ind. Electron.* 63 (7), 4495–4505. doi:10.1109/tie.2015.2508920

Ghosh, S., Rahman, S., and Pipattanasomporn, M. (2017). Distribution voltage regulation through active power curtailment with PV inverters and solar generation forecasts. *IEEE Trans. Sustain. Energy* 8 (1), 13–22. doi:10.1109/tste.2016.2577559

Hu, J, Shan, Y, Guerrero, J M., Adrian, I, Chan, K W, and Rodriguez, J (2021). Model predictive control of microgrids – an overview. *Renew. Sustain. Energy Rev.* 136, 110422. doi:10.1016/j.rser.2020.110422

Hu, J., Li, Y., and Zhu, J. (2019). Multi-objective model predictive control of doubly-fed induction generators for wind energy conversion. *IET Gener. Transm. &amp. Distrib.* 13, 21–29. doi:10.1049/iet-gtd.2018.5172

JacksonJusto, J, Mwasilu, F, Lee, J, and Jung, J-W (2013). AC-microgrids versus DC-microgrids with distributed energy resources: A review. *Renew. Sustain. Energy Rev.* 24, 387–405. doi:10.1016/j.rser.2013.03.067

Kumar, D., Zare, F., and Ghosh, A. (2017). DC microgrid Technology: System Architectures, AC grid interfaces, grounding schemes, power quality, communication networks, applications, and standardizations aspects. *IEEE Access* 5, 12230–12256. doi:10.1109/access.2017.2705914

Lashab, A., Sera, D., and Guerrero, J. M. (2019). A dual-discrete model predictive control-based MPPT for PV systems. *IEEE Trans. Power Electron.* 34 (10), 9686–9697. doi:10.1109/tpel.2019.2892809

Lashab, A., Sera, D., Guerrero, J. M., Mathe, L., and Bouzid, A. (2018). Discrete model-predictive-control-based maximum power point tracking for PV systems: Overview and evaluation. *IEEE Trans. Power Electron.* 33 (8), 7273–7287. doi:10.1109/tpel.2017.2764321

Liu, H., Loh, P. C., Wang, X., Yang, Y., Wang, W., and Xu, D. (2016). Droop control with improved disturbance adaption for a PV system with two power conversion stages. *IEEE Trans. Ind. Electron.* 63 (10), 6073–6085. doi:10.1109/tie.2016.2580525

Mahmood, H., Michaelson, D., and Jiang, J. (2015). Strategies for independent deployment and autonomous control of PV and battery units in islanded microgrids. *IEEE J. Emerg. Sel. Top. Power Electron.* 3 (3), 742–755. doi:10.1109/jestpe.2015.2413756

Meng, L., Shafiee, Q., Trecate, G. F., Karimi, H., Fulwani, D., Lu, X., et al. . (2017). Review on control of DC microgrids and multiple microgrid clusters. *IEEE J. Emerg. Sel. Top. Power Electron.* 5 (3), 928–948.

Nguyen, Q., Padullaparti, H. V., Lao, K., Santoso, S., Ke, X., and Samaan, N. (2019). Exact optimal power dispatch in unbalanced distribution systems with high PV penetration. *IEEE Trans. Power Syst.* 34 (1), 718–728. doi:10.1109/tpwrs.2018.2869195

Quevedo, D. E., Aguilera, R. P., Perez, M. A., Cortes, P., and Lizana, R. (2012). Model predictive control of an AFE rectifier with dynamic references. *IEEE Trans. Power Electron.* 27 (7), 3128–3136. doi:10.1109/tpel.2011.2179672

Shadmand, M. B., Balog, R. S., and Abu-Rub, H. (2014). Model predictive control of PV sources in a smart DC distribution system: Maximum power point tracking and droop control. *IEEE Trans. Energy Convers.* 29 (4), 913–921. doi:10.1109/tec.2014.2362934

Tonkoski, R, and Lopes, L A. C. (2011). Impact of active power curtailment on overvoltage prevention and energy production of PV inverters connected to low voltage residential feeders. *Renew. Energy* 36, 3566–3574. doi:10.1016/j.renene.2011.05.031

Ullah, S., Haidar, A. M. A., Hoole, P., Zen, H., and Ahfock, T. (2020). The current state of Distributed Renewable Generation, challenges of interconnection and opportunities for energy conversion based DC microgrids. *J. Clean. Prod.* 273, 122777. doi:10.1016/j.jclepro.2020.122777

Vicente, E. M., Vicente, P. D. S., Moreno, R. L., and Ribeiro, E. R. (2020). High-efficiency MPPT method based on irradiance and temperature measurements. *IET Renew. Power Gener.* 14 (6), 986–995. doi:10.1049/iet-rpg.2019.0849

Villalva, M. G., Gazoli, J. R., and Filho, E. R. (2009). Comprehensive approach to modeling and simulation of photovoltaic arrays. *IEEE Trans. Power Electron.* 24 (5), 1198–1208. doi:10.1109/tpel.2009.2013862

Wandhare, R. G., and Agarwal, V. (2011), "Advance control scheme and operating modes for large capacity centralised PV-grid systems to overcome penetration issues," in 2011 37th IEEE Photovoltaic Specialists Conference, 19-24 June 2011, Seattle, WA, USA, 2466–2471. doi:10.1109/PVSC.2011.6186445

Xiao, W., Dunford, W. G., Palmer, P. R., and Capel, A. (2007). Regulation of photovoltaic voltage. *IEEE Trans. Ind. Electron.* 54 (3), 1365–1374, Jun. doi:10.1109/tie.2007.893059